Attenuation of non-compressional energy in ocean bottom node data

Tim Seher[1]*, Hassan Masoomzadeh[1], Yong Ren[1], Fons ten Kroode[1], Mark Roberts[1], Alexander Kritski[2], Harald Westerdahl[2], Mark Thompson[2] and Åsmund Sjøen Pedersen[2] use rotational measurements from a new type of ocean bottom node for the attenuation of non-compressional energy.

Abstract

Attenuation of non-compressional energy, such as shear body waves and scattered surface waves, is a critical step in the processing of ocean bottom node seismic data, because this unwanted energy interferes with the desired compressional signals. In this paper, we first review conventional methods for attenuating non-compressional energy in vertical geophone recordings, including cooperative denoising procedures and adaptive subtraction techniques. We then introduce the use of rotational measurements from a new type of ocean bottom node for the attenuation of non-compressional energy. Our results demonstrate that rotational data improve the attenuation of the non-compressional energy, particularly for flat events at small offsets where conventional methods struggle. Finally, we explore the potential of machine learning to reduce the computational cost and human effort involved in the denoising workflow. Overall, the combination of conventional denoise techniques and rotational data delivers robust results. The introduction of machine learning provides a way forward that leverages the strengths of existing methods and reduces the cost of seismic data processing.

Introduction

The attenuation of undesired signals is a continuing issue in the processing of ocean bottom node (OBN) seismic data. An example is the presence of non-compressional energy on vertical geophone records (Paffenholz et al. 2006a, 2006b), which limits our ability to jointly process hydrophone and geophone data. This energy is linked to the presence of both shear body waves and scattered surface waves. It has been called interchangeably shear-wave noise, Vz noise (referring to noise on the vertical geophone), or more recently, non-compressional energy, a term that we will adopt here.

Over the years, a variety of processing techniques have been developed to attenuate non-compressional energy in vertical geophone recordings. The most common approach for attenuating non-compressional energy involves a cooperative denoising procedure between the vertical geophone and the hydrophone in different transform domains such as the Tau-p transform domain (Craft and Paffenholz 2007; Poole et al. 2012), the wavelet transform domain (Yu et al. 2011; Peng et al. 2013; Ren et al. 2020), and the curvelet transform domain (Yang et al. 2020; Kumar et al. 2021; Ren et al. 2022; Kumar et al. 2024). Recently, machine learning (ML) has been applied to accelerate non-compressional energy attenuation in vertical geophone recordings (Sun et al. 2023; Seher et al. 2024). However, a successful application of ML-based noise attenuation requires high-quality training data. New rotational sensors on the seafloor (Pedersen et al. 2023; Kritski et al. 2024; Masoomzadeh et al. 2024) are expected to provide appropriate training data for this purpose.

In this paper, we first review four solutions for the attenuation of non-compressional energy in OBN recordings, then demonstrate that rotational records from a prototype receiver can be used to improve the denoising process, and finally show how ML can be utilised to reduce the computational cost and the human effort involved in the noise attenuation workflow.

Conventional methods for the attenuation of non-compressional energy

A major problem with separating hydrophone and geophone recordings into upgoing and downgoing wavefields is the presence of strong non-compressional energy in the vertical geophone records. Different methods have been developed to attenuate this unwanted energy in OBN recordings. These methods commonly exploit two different properties of multi-component data. The first property is that non-compressional energy is not detected by the hydrophone. This property allows the attenuation of non-compressional energy in the vertical geophone data by using the hydrophone data as a guide in a cooperative denoising process. The second property is that horizontal geophones are more sensitive to non-compressional motions. Using the horizontal recordings as noise models allows for the attenuation of this noise by simultaneous adaptive subtraction. Here, we will be comparing four methods for the attenuation of non-compressional energy based on the 2D dual-tree complex wavelet transform, both 2D and 3D curvelet transforms, and the simultaneous adaptive subtraction of data recorded by horizontal geophones.

We start by showing results for one of these methods based on the 3D curvelet transform (Figure 1). The curvelet domain is attractive for noise attenuation because it allows a detailed frequency and

[1] TGS | [2] Equinor
* Corresponding author, E-mail: tim.seher@tgs.com
DOI: 10.3997/1365-2397.fb2024106

orientation dependent representation of the data, where noise and signal can be distinguished. To exploit this property, we first transform both hydrophone and geophone records of a receiver gather from a survey in the Gulf of Mexico into the 3D curvelet domain. In this domain, thresholding based on the ratio of the curvelet coefficients allows the conservation of events that are present in both hydrophone and vertical geophone data and then the attenuation of those events that are only present in the vertical geophone records. In the curvelet domain, the algorithm naturally honours the dip and frequency content of the input data. The thresholding step yields a noise model that can be inverse transformed back to the offset domain. Subtraction of the noise model from the input data removes non-compressional energy and gives the desired compressional signal. In addition, we would like to point out that the curvelet domain is not only suitable for the attenuation of non-compressional energy, but also facilitates additional processing steps including deblending, data dependent obliquity correction, and calibration of hydrophone and geophone measurements.

To better understand the benefits and drawbacks of the methods described above, we apply these methods to the data from one receiver and compare the resulting noise models (Figure 2). We start by comparing methods based on both 2D wavelet and 2D curvelet transforms, which internally use a similar thresholding scheme. Two passes of the 2D curvelet method (in both inline and crossline directions) yield a more coherent noise model than two passes of the 2D wavelet transform method (Figures 2a&b). Furthermore, our 2D curvelet-based method better preserves the desired signals. This may be due to a finer dip sampling in the curvelet domain. A comparison of two passes of the 2D curvelet approach with a full 3D curvelet approach (Figures 2b&c) shows that the 3D method better preserves event continuity and leaves fewer artifacts and less noise. Finally, we compare the 3D curvelet method with simultaneous adaptive subtraction. In this approach, we adaptively subtract the two horizontal geophones from the vertical geophone while using the hydrophone data to protect the desired signal. This comparison shows that both approaches yield noise models with coherent shear events (Figures 2c&d). However, the 3D curvelet noise model has captured additional incoherent energy.

Attenuation of non-compressional energy using rotational measurements

Conventional OBN data processing involves the separation of upcoming and downgoing wavefields. A successful separation requires high-quality compressional signals captured in both pressure and vertical motion records. A frequent problem is that the vertical sensor captures non-compressional energy corresponding to both shear and surface waves. This energy needs to be attenuated prior to acoustic wavefield separation. The conventional approaches described in the previous section are successful for dipping events at large offsets but are less effective in the near offset zone for flat events. That is because around the apex both compressional and non-compressional events appear flat, and therefore become less distinguishable in the transform domain.

A conventional OBN survey contains data from four receivers: a hydrophone to record pressure, and three orthogonal geophones to record particle velocity. During the Amendment 2 OBN survey, in addition to the conventional four-component nodes, we acquired seismic data using two test nodes equipped with a new sensor type (Pedersen et al. 2023; Masoomzadeh et al. 2024). This new generation node contains a hydrophone and

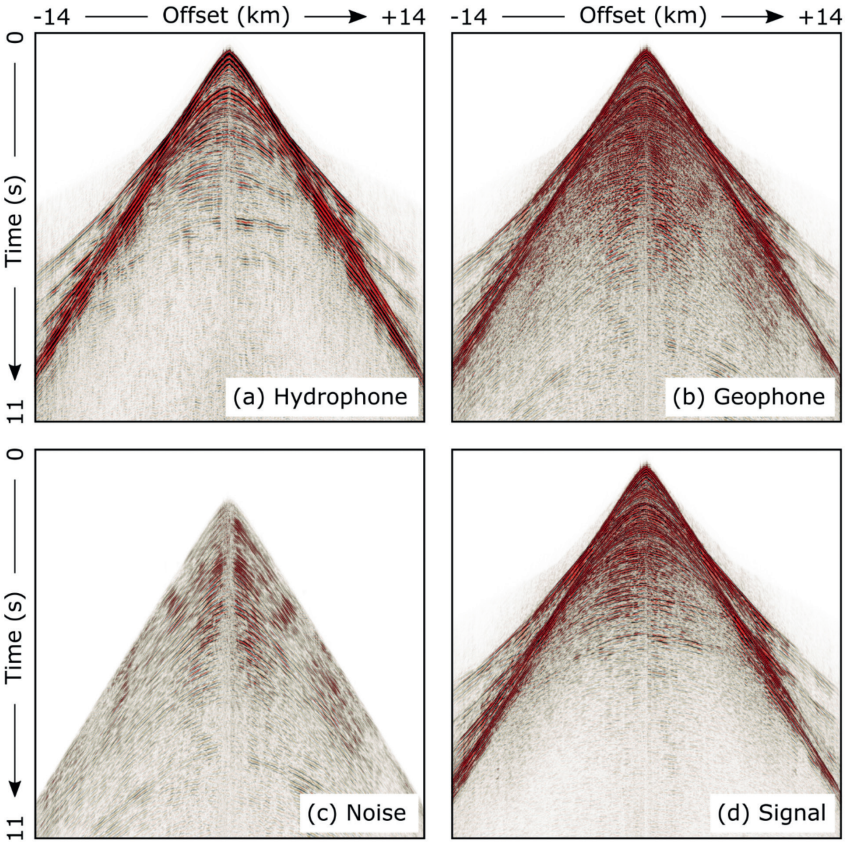

Figure 1 3D curvelet denoising uses the hydrophone record (a) to attenuate converted body waves and surface waves in the vertical geophone record (b). This process decomposes the input geophone data into a signal model (d) and a noise model (c). The figures shown here come from a conventional four-component OBN and were created by averaging traces for a given offset within a 45° azimuth angle range.

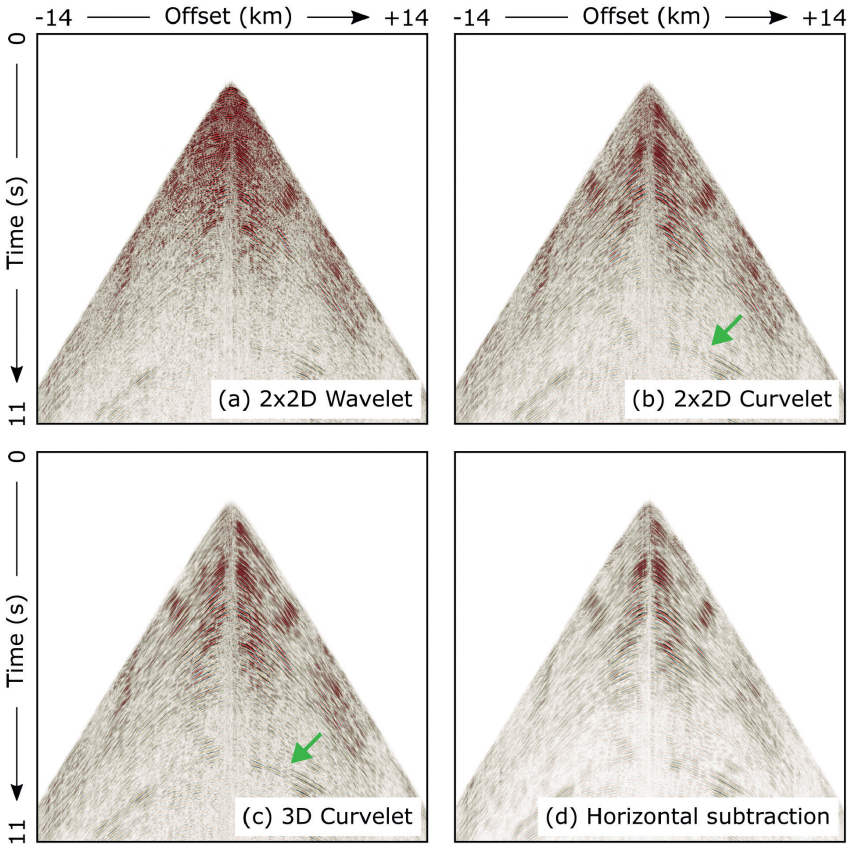

Figure 2 Noise models estimated using a two-pass 2D wavelet transform (a), a two-pass 2D curvelet transform (b), a single pass 3D curvelet transform (c), and simultaneous adaptive subtraction of horizontal geophones from the vertical geophone (d). The arrows highlight areas where the 3D approach has removed more coherent energy than the two-pass 2D approach. The noise models correspond to the data shown in Figure 1, and traces were averaged for a given offset within a 45° azimuth angle range.

six additional sensors. These six sensors are made of piezoelectric crystals mounted on the faces of a solid cubic frame, holding a metal sphere acting as an inertial mass. The crystals and the electronic circuit attached to them are designed to record voltages proportional to particle acceleration in a specific direction. Crucially, a summation of output voltages from two parallel crystals on opposite faces of the cubic frame provides one component of the translational acceleration vector, while a subtraction of those outputs provides a component of the rotational acceleration vector in a perpendicular direction. In combination, this new generation node provides measurements of pressure, the full translational acceleration vector, and the full rotational acceleration vector.

An interesting property of the acquired rotational data is the absence of compressional energy in these recordings. The reason is that a pressure signal propagates by displacing particles in the propagation direction, meaning that those particles do not experience any rotations. For a better understanding, imagine holding a sponge ball in the palm of your hand, and an imaginary multi-sensor receiver is present inside the ball. You may try the following actions to simulate compressional, shear and surface waves. First, squeeze the ball while maintaining its position and orientation. A hydrophone can tell you how firmly you are squeezing. Second, move the ball around without squeezing or changing its orientation. A set of orthogonal geophones can tell the speed and direction of those translational motions. Finally, roll the ball without squeezing or changing its location. A conventional node is oblivious to those rotational motions. Hence, the new sensor has been constructed to measure both translational and rotational acceleration vectors.

In the above experiment, we may notice that squeezing the ball does not change its orientation. This implies that pressure signals should not be detected by a sensor that is designed to detect only rotational motions. Therefore, acquiring rotational data is particularly helpful for the purpose of separating compressional and non-compressional events appearing in the vertical translational component. Although the rotational sensors have successfully captured non-compressional energy, the recorded rotational signals are not identical to the non-compressional signals captured in the vertical translational record. Rotational records may be considered as spatial derivatives of translational records. In theory, we need to convert horizontal rotational data (i.e., rotations around the two horizontal axes) to simulate vertical translational data. We derived a formula for this conversion (Masoomzadeh et al. 2024) based on a flat earth assumption. Because of this assumption, it is only kinematically correct. To address the dynamic variations, we used simultaneous adaptive subtraction to optimally match two horizontal rotational components to the vertical translational component and subtracted them from it.

To illustrate the advantages of the new data, we first present a data example together with the results from the proposed processing sequence (Figures 3&4). Comparing the hydrophone and vertical acceleration (Figures 3a&b) shows the presence of significant non-compressional energy on the vertical receiver in addition to the desired compressional energy. Comparing the vertical acceleration and the horizontal rotation shows that the rotational sensors capture non-compressional energy exclusively. This property makes the rotational data an ideal noise model for the adaptive subtraction (Figure 4b).

Comparing the results of the adaptive subtraction of horizontal geophones with the results of the previously presented 3D curvelet method allows interesting insights (Figures 4a&b). The adaptive

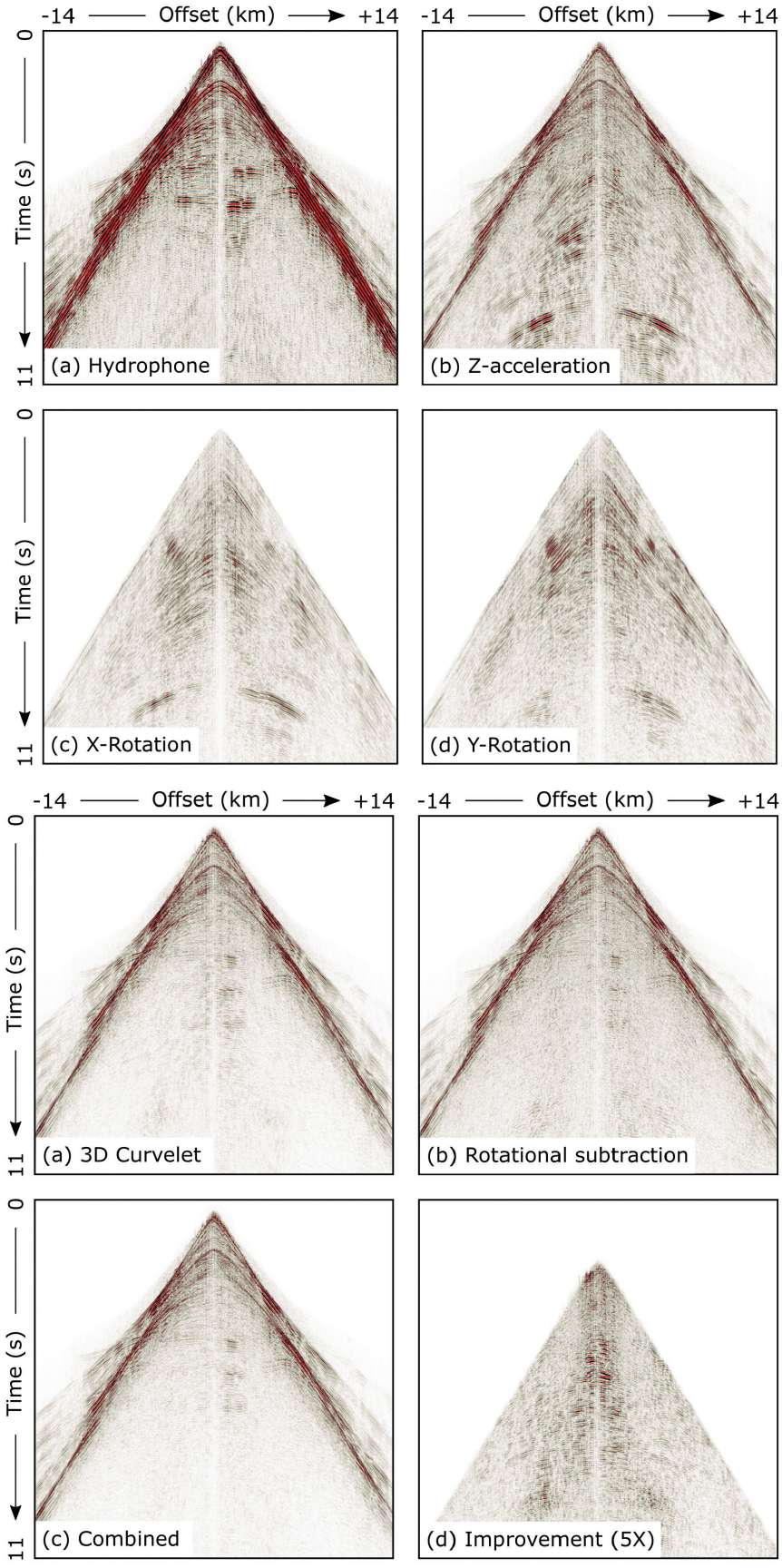

Figure 3 Four of the seven recorded components from the novel OBN receiver deployed in the Gulf of Mexico. The hydrophone, vertical accelerometer, and the sensors measuring rotation around the x- and y-axis of the instrument were used in our noise attenuation processing sequence. The data correspond to a 45° stack for positive or negative offsets, respectively. Hydrophone, acceleration and rotation data have different ranges and are scaled independently.

Figure 4 Vertical acceleration after application of 3D curvelet denoise only (a), after simultaneous adaptive subtraction of the rotational measurements only (b), and the combined application of both methods (c). The difference between only applying 3D curvelet denoise and applying both adaptive subtraction and curvelet denoise demonstrates the improvement possible by combining the two techniques (d). The differences (d) are scaled up by a factor of 5. The results correspond to the data shown in Figure 3.

subtraction method successfully attenuates non-compressional energy in the near offset zone, where the curvelet method is less successful. The curvelet method successfully attenuates dipping non-compressional events, but it is less successful at attenuating flat parts of those undesired events at near offsets. A combination of the two methods (Figures 4c&d) removes more noise than each individual method.

Role of machine learning in non-compressional energy attenuation

The conventional methods of non-compressional energy attenuation presented above allow separating compressional and non-compressional signals in OBN data. However, these methods can be hard to parameterise for the user and costly to apply in terms of computational resources. In recent years, ML solutions have been deployed for different seismic processing tasks including the attenuation of non-compressional energy in OBN data (Sun et al. 2023; Seher et al. 2024). These ML solutions allow significant reduction of computational cost, if the up-front cost of training the ML network is ignored. In addition, pre-trained networks minimise the human effort during processing.

To illustrate the potential of ML in the attenuation of non-compressional energy, we trained a network using seismic data from two regions in the North Sea including the area North of Alvheim Krafla Askja (NOAKA). We then applied the denoising network to a line of receivers from the NOAKA region that was not included as part of the training data. Comparing the ML results with the curvelet results for a single holdout receiver (Figure 5) allows a few interesting observations. First, the ML solution has not learned the transform artifacts apparent in the curvelet results. Second, the ML results are more conservative than the curvelet results – we observe less primary damage but more high-frequency noise in the signal display. Furthermore, the brute stack results for an entire receiver line (Figures 6a&b) demonstrate that the ML solution has successfully attenuated a significant amount of noise. Comparing the stacks of noise models for the curvelet and ML solutions (Figures 6c&d) demonstrates again that the ML solution is more conservative than the training data. Interestingly, the ML solution has removed additional noise at the beginning of the profile that was not removed by the curvelet method. This behaviour is due to the diversity of the training data and would be difficult to imitate by a human.

The conventional noise attenuation methods presented here can be used to create high-quality training data, which allows progress both in the short and long term. In the short term, training data can be created for each experiment separately, using a subset of receivers. Application of this customised network to all receivers for a single experiment has the potential to bring down the computational cost. In the long term, with the availability of

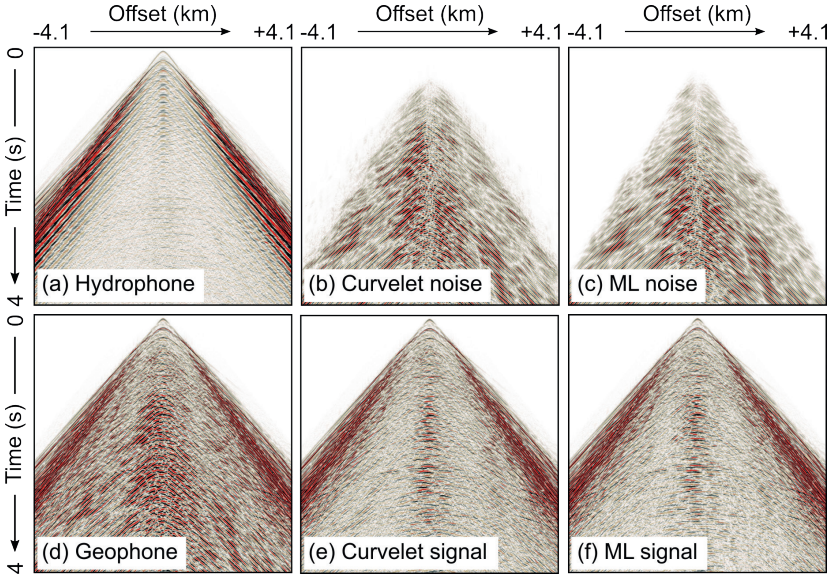

Figure 5 Comparison of 2D curvelet non-compressional energy attenuation and ML-based noise attenuation for a hold-out receiver. The curvelet and ML noise models (b&c) are qualitatively similar and a comparison of the signal models (e&f) to the vertical geophone (d) shows significant noise reduction for both methods.

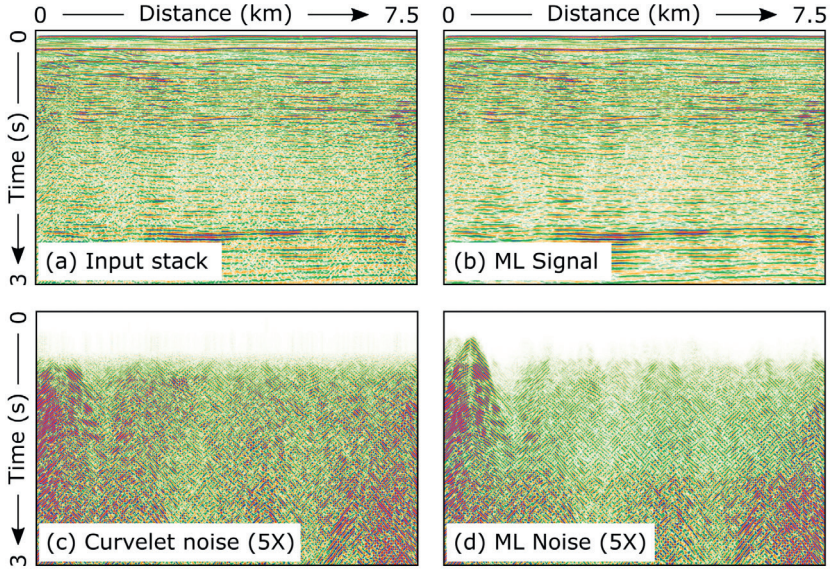

Figure 6 Comparison of a brute stack before and after ML denoise (a&b). The differences between curvelet and ML denoise (c&d) show that ML denoise is overall more conservative but can be more flexible with respect to variable noise content. The noise stacks are scaled by a factor of 5 compared to the signal stacks.

sufficient training data, we may be able to utilise a generalised network, at least as part of a fast-track processing workflow.

Finally, we have demonstrated that non-compressional energy attenuation is improved when the nodes are equipped with rotational sensors. The extra measurements of particle motions at the seabed can help to improve noise attenuation, and thereby provide superior training data for ML applications. This is of particular interest because we may only have to deploy the rotational sensors on a sparse grid to achieve the goal of improved denoising. The use of rotational data for ML applications will be a topic of future research.

Conclusions

Removing unwanted non-compressional energy such as surface waves and shear body waves from vertical motion recordings in OBN data is a critical step in acoustic wavefield processing, because this energy often interferes with the desired compressional signals. In this paper, we first reviewed conventional methods of attenuating this energy while highlighting their strengths and weaknesses. We then presented two significant advances – the use of rotational data and the application of ML methods.

While the conventional methods are effective overall in attenuating non-compressional energy, they struggle with the attenuation of flat events at near offsets. This shortcoming can be addressed by using a new type of receiver that measures the rotational accelerations. These rotational measurements can be treated as a noise model and adaptively subtracted from the translational data. This method allows the attenuation of non-compressional events that are not distinguishable based on dip or frequency. Furthermore, combining conventional techniques with adaptive subtraction of rotational data provides superior denoising results.

Finally, we explored the potential of ML for the attenuation of non-compressional energy and argued that ML can significantly reduce the computational cost and human effort. Crucially, we demonstrated the applicability of ML solutions for non-compressional energy attenuation as part of fast-track processing and showed its potential of outperforming a human data processor. In general, many ML techniques require the availability of high-quality and diverse training data. Relying on conventional processing solutions to generate these training data introduces subjectivity and error sources. Directly measuring the desired noise labels using rotational measurements has the promise of delivering superior training data and hence improving the noise attenuation results.

Acknowledgements

We are grateful to the many colleagues who contributed to this research. We would also like to thank TGS management and our joint venture partner SLB for permission to show the data.

References

Craft, K.L. and Paffenholz, J. [2007]. Geophone noise attenuation and wavefield separation using a multidimensional decomposition technique. *SEG Technical Program*, Expanded Abstracts, 2630-2634. https://doi.org/10.1190/1.2793013

Kritski, A., Westerdahl, H., Pedersen, Å.S., Thompson, M., Kroode, F.T., Seher, T. and Bernitsas, N. [2024]. Efficient Vz Noise suppression by seismic polarization analysis of 6C seabed data. *Fourth EAGE Marine Acquisition Workshop*, Extended Abstracts. https://doi.org/10.3997/2214-4609.202436003

Kumar, A., Hampson, G. and Rayment, T. [2021]. Simultaneous up-down separation and Vz denoise using joint sparsity recovery. *82nd EAGE Annual Conference & Exhibition*, Extended Abstracts. https://doi.org/10.3997/2214-4609.202112695

Kumar, R., Amin, Y.I.K., Leake, S., Vassallo, M., Bagaini, C., Sonika, S., Scapin, D. and De Melo, F.X. [2024]. Shear noise attenuation using multidimensional optimum Bayesian weighting. *85th EAGE Annual Conference & Exhibition*, Extended Abstracts. https://doi.org/10.3997/2214-4609.2024101142

Masoomzadeh, H., ten Kroode, F., Seher, T., Zuberi, M.A.H., Kritski, A., Westerdahl, H., Pedersen, Å.S., Thompson, M., Bernitsas, N., Behn, P. and Baltz, P. [2024]. Attenuating non-compressional energy on vertical motion sensors using rotational data. *Fourth International Meeting for Applied Geoscience & Energy*, Expanded Abstracts.

Paffenholz, J., Shurtleff, R., Hays, D. and Docherty, P. [2006a]. *Shear wave noise on OBS Vz data – Part I Evidence from field data*. 68th EAGE Annual Conference and Exhibition incorporating SPE EUROPEC 2006, cp-2-00235. https://doi.org/10.3997/2214-4609.201402227

Paffenholz, J., Docherty, P., Shurtleff, R. and Hays, D. [2006b]. *Shear wave noise on OBS Vz data – Part II Elastic modeling of scatterers in the seabed*. 68th EAGE Conference and Exhibition incorporating SPE EUROPEC 2006, cp-2-00236. https://doi.org/10.3997/2214-4609.201402228

Pedersen, Å.S., Kritski, A., Westerdahl, H., Thompson, M., David, S., Kroode, F.T., Bernitsas, N., Olivier, A., Behn, P., Baltz, P., Faber, K., Tatarata, A., Barry, R. and Greco, M., [2023]. Towards a next generation ocean bottom node: Incorporating a 6C motion sensor. *84th EAGE Annual Conference & Exhibition*, Extended Abstracts. https://doi.org/10.3997/2214-4609.202310476

Peng, C., Huang, R. and Asmerom, B. [2013]. Shear noise attenuation and PZ matching for OBN data with a new scheme of complex wavelet transform. *SEG Technical Program*, Expanded Abstracts, 4251-4255. https://doi.org/10.1190/segam2013-0634.1

Poole, G., Casasanta, L. and Grion, S. [2012]. Sparse τ-p Z-noise attenuation for ocean-bottom data. *SEG Technical Program*, Expanded Abstracts, 1-5. https://doi.org/10.1190/segam2012-0679.1

Ren, Y., Yang, C., Degel, T. and Liu, Z. [2020]. Vz noise attenuation using dual-tree complex wavelet transform. *SEG Technical Program*, Expanded Abstracts, 1830-1834. https://doi.org/10.1190/segam2020-3426428.1

Ren, Y., Yang, C., Seher, T., Hawke, M. and Cho, E. [2022]. Vz denoise and P/Z matching in 3D curvelet domain. *SEG Technical Program*, Expanded Abstracts, 2862-2866. https://doi.org/10.1190/image2022-3745669.1

Seher, T., Yalcin, G., Roberts, M. and Ren, Y. [2024]. Shear wave noise attenuation in ocean bottom node data using machine learning. *85th EAGE Annual Conference & Exhibition*, Extended Abstracts. https://doi.org/10.3997/2214-4609.202410498

Sun, J., Jafargandomi, A. and Holden, J. [2023]. Deep learning-based Vz-noise attenuation for OBS data, *SEG Technical Program*, Expanded Abstracts, 1480-1484. https://doi.org/10.1190/image2023-3910189.1

Yang, C., Huang, Y., Liu, Z., Sheng, J. and Camarda, E. [2020]. Shear wave noise attenuation and wavefield separation in curvelet domain. *SEG Technical Program*, Expanded Abstracts, 1805–1809. https://doi.org/10.1190/segam2020-3426418.1

Yu, Z., Kumar, C. and Ahmed, I. [2011]. Ocean bottom seismic noise attenuation using local attribute matching filter, *SEG Technical Program*, Expanded Abstracts, 3586–3590. https://doi.org/10.1190/1.3627945